Substitution of Equations (A6) and (A7) into (A5) gives after simplification

$$\ln(f/f^*) = -\ln(g/g^*) + Z - 1 \qquad (A8)$$

From the definition it can be shown that g^* is equal to the volume. The fugacity of an ideal gas f^* is simply the pressure. It must be noted however that an ideal gas and a nonideal gas at the same temperature and molar volume cannot have the same pressure. This fact leads to the following relationship

$$f^* = P^* = P/Z \qquad (A9)$$

Substitution for f^* and g^* in Equation (A8) gives the desired result.

$$\ln(Zf/P) = -\ln(g/V) + Z - 1 \qquad (A10)$$

Manuscript received March 30, 1971; revision received August 11, 1971; paper accepted August 16, 1971.

II. Prediction of Component Fugacities and Related Properties of Mixtures

W. R. LEYENDECKER and R. D. GUNN

Department of Chemical Engineering
University of Texas, Austin, Texas 78712

A computer program based on the theory of Part I is developed for calculating equilibrium ratios and related thermodynamic properties of mixtures, and a variety of data are used to test the method. For the carbon dioxide-*n*-butane system both liquid and gaseous compressibility factors are predicted with an average absolute deviation from experimental values of 1.3% for a wide range of conditions. A maximum deviation of 5.4% occurs in the critical region. Derivative properties such as component fugacities and equilibrium ratios show somewhat larger deviations as expected. For the same system average deviations are 2.7% for carbon dioxide fugacities, 2.6% for *n*-butane fugacities, and 3.3% for carbon dioxide and *n*-butane equilibrium ratios. Average deviation for predicted equilibrium ratios for eight binary systems and 574 data points is 4.6%. Equilibrium ratios for two ternary systems are also predicted accurately. The major advantage of the method, however, is the small or negligible amount of experimental mixture data required. The method has not been tested below a mixture reduced temperature of 0.8, the lower limit of the Pitzer tables. Without density corrections to the scaling parameters best results are obtained if all binary pairs in a mixture fall within range $0.25 < V_{Cj}\,T_{Cj}/V_{Ci}\,T_{Ci} < 4.0$.

In Part I a method founded on the principle of corresponding states is developed for predicting component fugacities and related thermodynamic properties of dense fluid mixtures. An accurate method for calculating the fugacity of a component is especially important for the prediction of phase equilibria. Equation (35) defines the criterion for equilibrium between a gaseous and a liquid phase involving any number of components.

$$f_{iG} = f_{iL} \qquad (35)$$

In a multicomponent mixture, a separate relationship, each of the same form as Equation (35), is obeyed by each component. The problem of predicting vapor-liquid equilibria, therefore, is resolved into one of predicting the temperature, pressure, and composition dependence of the component fugacities. Such predictions are possible through the use of Equation (34).

DERIVATIVES OF THE SCALING PARAMETERS

Equation (34) requires the derivatives of the scaling parameters with respect to composition. These derivatives for the scaling volume and the mixture acentric factor are readily derived from Equations (6) and (8)

$$\left(\frac{\partial V_{CM}}{\partial y_i}\right)_{\substack{\text{all } y_j \\ j\neq i}} = 2\sum_{j=1}^{N} y_j\, V_{Cij} \qquad (36)$$

$$\left(\frac{\partial \omega_M}{\partial y_i}\right)_{\substack{\text{all } y_j \\ j\neq i}} = \frac{2}{V_{CM}}\sum_{j=1}^{N} y_j\,(\omega_{ij} - \omega_M)\,V_{Cij} \qquad (37)$$

As with Equation (25) the composition derivatives are taken with the temperature, the molal volume, and all but one mole fraction being held constant. The derivative of the scaling temperature is obtained from Equation (9).

$$V_{CM}\frac{\partial B_{RM}}{\partial T_{RM}}\left(\frac{\partial T_{RM}}{\partial y_i}\right)_{\substack{T,\text{ all } y_j \\ j\neq i}} + V_{CM}\,B^1{}_{RM}\left(\frac{\partial \omega_M}{\partial y_i}\right)_{\substack{\text{all } y_j \\ j\neq i}}$$

$$+ B_{RM}\left(\frac{\partial V_{CM}}{\partial y_i}\right)_{\substack{\text{all } y_j \\ j\neq i}} = 2\sum_{j=1}^{N} y_j\,B_{Rij}\,V_{Cij} \qquad (38)$$

The desired relationship is obtained after substitution of Equation (32) into (38) and after further rearrangement:

Correspondence concerning this paper should be addressed to R. D. Gunn at the University of Wyoming, Laramie, Wyoming 82070.

$$\frac{1}{T_{CM}}\left(\frac{\partial T_{CM}}{\partial y_i}\right)_{\substack{\text{all } y_j \\ j\neq i}} = \frac{\dfrac{B_{RM}}{V_{CM}}\left(\dfrac{\partial V_{CM}}{\partial y_i}\right)_{\substack{\text{all } y_j \\ j\neq i}} + B^1{}_{RM}\left(\dfrac{\partial \omega_M}{\partial y_i}\right)_{\substack{\text{all } y_j \\ j\neq i}} - \dfrac{2}{V_{CM}}\sum_{j=1}^{N} y_j B_{Rij} V_{Cij}}{T_R\,(\partial B_{RM}/\partial T_R)} \tag{39}$$

Equations (36), (37), and (39) require definitions for V_{Cij}, ω_{ij}, and T_{Cij} for the situation when i is not equal to j. In principle these reducing parameters may be calculated from experimental cross second virial coefficients from the equation

$$B_{ij} = B_{Rij}\,V_{Cij} = \left[\, B^0{}_{Rij}\left(\frac{T}{T_{Cij}}\right) + \omega_{ij}\,B^1{}_{Rij}\left(\frac{T}{T_{Cij}}\right)\right] V_{Cij} \tag{40}$$

The generalized functions for $B^0{}_{Rij}$ and $B^1{}_{Rij}$, Equations (4) and (5), are the same as those used for pure components. In practice the experimental data for cross second virial coefficients are seldom sufficiently accurate or available over a sufficiently wide temperature range to permit the calculation of three parameters simultaneously. Therefore, we rather arbitrarily select the following combining rules for V_{Cij} and ω_{ij}:

$$V_{Cij} = 1/2\,(V_{Ci} + V_{Cj}) \tag{41}$$

$$\omega_{ij} = \frac{\omega_i V_{Ci} + \omega_j V_{Cj}}{V_{Ci} + V_{Cj}} \tag{42}$$

For T_{Cij} we adopt the following relationship which has been used by a number of other investigators (*20* to *25*, Part I).

$$T_{Cij} = (1 - k_{ij})\,(T_{Ci}\,T_{Cj})^{1/2} \tag{43}$$

The constant k_{ij} is a true binary parameter and for best accuracy it must be obtained from experimental binary mixture data. It is the only mixture parameter used in this development. Chueh and Prausnitz (*1*) have tabulated values of k_{ij} for over a hundred binaries. Additional k_{ij}'s have been tabulated by others (*24*, *25*, Part I). When experimental or tabulated k_{ij}'s are lacking they may be calculated from a new relationship developed by Hiza and Duncan (*25*, Part I) which requires pure component data only.

GENERALIZED FUNCTIONS

A computer program has been prepared for the calculation of component fugacities by the method described. This method uses several generalized thermodynamic functions which are obtained from the Pitzer tables contained in the program. First a reduced temperature and pressure and an acentric factor are calculated for the mixture from Equations (9), (10), and (8) respectively. With these parameters the fugacity coefficient and the compressibility factor for the mixture are readily evaluated from the appropriate generalized tables. The internal energy departure is computed from the relationship

$$\frac{U_M^* - U_M}{RT_{CM}} = \frac{H_M^* - H_M}{RT_{CM}} + T_{RM}(Z_M - 1) \tag{44}$$

The final mixture property required is the function $\ln(g_M/V_M)^1$, defined by Equation (18), for which no generalized tables exist. An approximation of this function, however, is derived from Equation (19).

$$\ln\left(\frac{f}{P}\right)^0 + \omega \ln\left(\frac{f}{P}\right)^1 + \ln\,(Z^0 + \omega Z^1) + 1 - Z^0 - \omega Z^1 = -\ln\,(g/V)^0 - \omega \ln\,(g/V)^1 \tag{45}$$

$$\ln\,(f/P)^0 + \ln Z^0 + 1 - Z^0 = -\ln\,(g/V)^0 \tag{46}$$

Equation (45) corresponds to a fluid with a measurable acentric factor and Equation (46) to a simple fluid. Subtraction of (46) from (45) gives the desired result.

$$-\ln\left(\frac{g_M}{V_M}\right)^1 = \ln\left(\frac{f_M}{P}\right)^1 + \frac{1}{\omega_M}\ln\left(1 + \frac{\omega_M Z_M{}^1}{Z_M{}^0}\right) - Z_M{}^1 \tag{47}$$

Equation (47) is only an approximation. This follows from the fact that $\ln\,(g/V)^1$ is the first-order coefficient in a Taylor series expansion of the configuration potential about the acentric factor.

$$\ln\,(g/V) = \ln\,(g/V)_{\omega=0} + \left(\frac{\partial \ln\,(g/V)}{\partial \omega}\right)_{\substack{T_R,\,V_R \\ \omega=0}} \omega + (1/2!)\left(\frac{\partial^2 \ln\,(g/V)}{\partial \omega^2}\right)_{\substack{T_R,\,V_R \\ \omega=0}} \omega^2 + \cdots \tag{48}$$

The formal definition of $\ln\,(g/V)^1$ therefore comes directly from the Taylor series, Equation (48).

$$\ln\,(g/V)^1 = \left[\frac{\partial \ln(g/V)}{\partial \omega}\right]_{\substack{T_R,\,V_R \\ \omega=0}} \tag{49}$$

$\ln\,(g/V)^1$ is defined at constant reduced volume whereas $\ln\,(f/P)^1$ and Z^1 are defined by Pitzer et al. (*2*, Part I) at constant reduced pressure

$$\ln\,(f/P)^1 = \left[\frac{\partial \ln(f/P)}{\partial \omega}\right]_{\substack{T_R,\,P_R \\ \omega=0}} \tag{50}$$

$$Z^1 = \left(\frac{\partial Z}{\partial \omega}\right)_{\substack{T_R,\,P_R \\ \omega=0}} \tag{51}$$

The relationship between Equation (50) and a constant volume derivative is obtained from the chain rule of differentiation.

$$\ln\,(f/P)^1 = \left(\frac{\partial \ln f/P}{\partial \omega}\right)_{\substack{T_R,\,P_R \\ \omega=0}} = \left(\frac{\partial \ln f/P}{\partial \omega}\right)_{\substack{T_R,\,P_R \\ \omega=0}} + \left(\frac{\partial \ln f/P}{\partial V_R}\right)_{\substack{T_R,\omega \\ \omega=0}} \left(\frac{\partial V_R}{\partial \omega}\right)_{\substack{T_R,\,P_R \\ \omega=0}} \tag{52}$$

Equation (52) shows that the use of tables of $\ln\,(f/P)^1$, which are the constant pressure derivatives, in place of the

required constant volume derivatives results in the neglect of the term

$$\left(\frac{\partial \ln f/P}{\partial V_R}\right)_{\substack{T_R,\omega \\ \omega=0}} \left(\frac{\partial V_R}{\partial \omega}\right)_{\substack{T_R,\,P_R \\ \omega=0}}$$

Similar arguments apply to Z^1 as well. For gases the neglected quantities are second order. For liquids the error becomes larger, and below a reduced temperature of 0.8 these terms must be taken into consideration. Partly for this reason calculations presented in this paper are limited to reduced temperatures of the liquid mixture above 0.8.

Table 1 outlines the computational procedure just discussed for vapor-liquid equilibrium calculations.

TABLE 1. COMPUTATIONAL PROCEDURE FOR VAPOR-LIQUID EQUILIBRIUM CALCULATIONS

Step No.	Remarks or procedure	Equations used
1.	Initiate trial values of liquid and vapor mole fractions	—
2.	Calculate V_{Cij}, ω_{ij}, T_{Cij}	(41), (42), (43)
3.	Calculate V_{CM}, ω_M for vapor	(6) (8)
4.	Calculate T_{CM} for vapor (by iteration)	(4), (5), (9)
5.	Calculate Z_{CM}, P_{CM} for vapor	(11), (10)
6.	Calculate $\frac{H_M^* - H_M}{RT_{CM}}$, Z_M^0, Z_M^1, $\ln(f_m/P)^1$, with T_{CM}, P_{CM} and ω_M	Pitzer Tables
7.	Calculate $\frac{U_M^* - U_M}{RT_{CM}}$	(44)
8.	Calculate $\ln(g_M/V_M)^1$	(47)
9.	Calculate $\frac{\partial V_{CM}}{\partial y_i}$, $\frac{\partial V_{CM}}{\partial y_j}$	(36)
10.	Calculate $\frac{\partial \omega_M}{\partial y_i}$, $\frac{\partial \omega_M}{\partial y_j}$	(37)
11.	Calculate $\frac{\partial T_{CM}}{\partial y_i}$, $\frac{\partial T_{CM}}{\partial y_j}$	(3), (4), (5), (39)
12.	Calculate $\ln(f_i/y_iP)$ for each component	(34)
13.	Repeat steps (3) to (12) to calculate $\ln(f_i/x_iP)$ for each component in the liquid phase	—
14.	From $\ln(f_i/y_iP)$ and $\ln(f_i/x_iP)$ calculate new compositions y_i and x_i	(35)
15.	Reiterate steps (3) to (14) until convergence is obtained for mole fractions y_i and x_i	—

LIMITATIONS

The theoretical development of the proposed method involves the assumption that the mixture scaling parameters are independent of density. From theoretical considerations it is expected that this assumption fails whenever the size differences between the different molecular species in the mixture become very large. This limitation is found to be important in practice as well. A rough but convenient measure of these size differences and the accompanying differences in the molecular force fields is the ratio $V_{Cj}\,T_{Cj}/V_{Ci}\,T_{Ci}$. We find that thermodynamic data calculated by the method proposed becomes increasingly inaccurate whenever the ratio $V_{Cj}\,T_{Cj}/V_{Ci}\,T_{Ci}$ falls outside of the range 0.25 to 4.0 for a binary pair in the mixture.

A second limitation of the method results from the fact that the Pitzer Tables of thermodynamic properties do not extend to reduced temperatures lower than 0.8.

COMPARISON OF RESULTS: BINARY MIXTURES

The carbon dioxide-*n*-butane system is selected for a primary role in determining the capabilities of the proposed method. Mixtures of carbon dioxide and hydrocarbons are known to exhibit anomalous thermodynamic behavior when compared to mixtures of hydrocarbons only, and the ability to predict phase behavior of these systems serves a valuable purpose. Fortunately, a wide variety of data are available for saturated gaseous and liquid mixtures of carbon dioxide and *n*-butane (2). These data include liquid and gaseous compressibility factors, vapor-liquid equilibrium measurements, and component fugacities. Component fugacities are especially valuable for comparative purposes, but they are available for only a few systems. Table 2 shows a comparison between calculated and experimental results for this system.

Only deviations for the 160°F. isotherm are shown in Table 2. This isotherm is representative of the system as a whole because of the wide range of pressure and composition exhibited along the two phase locus at this temperature.

Average deviations for calculated equilibrium ratios spanning the temperature range of 100° to 220°F. are summarized in Table 3. For the butane-carbon dioxide system the computations, upon which this table is based, show large anomalous deviations (10 to 20% for component fugacities) for liquid data at 280°F. but show good agreement for the gaseous phase at the same temperature. An integral thermodynamic consistency test shows that the gas phase data are consistent but that liquid data are not. For this reason deviations of butane and carbon dioxide equilibrium ratios at 280°F. are not included in the results reported in Table 3.

TABLE 2. COMPARISON OF SEVERAL THERMODYNAMIC PROPERTIES (CALCULATED BY THE CORRESPONDING STATES METHOD) WITH EXPERIMENTAL VALUES FOR THE CARBON DIOXIDE-*n*-BUTANE SYSTEM AT 160°F.

		Mole fraction carbon dioxide		Compressibility factors				Fugacities for CO_2			Fugacities for *n*-butane			Equilibrium ratios			
				Sat. liq.		Sat. gas		Exp.	Calc. values		Exp.	Calc. values		Carbon dioxide		*n*-butane	
Temp.	press.	Gas phase	Liquid phase	Exp.	Calc. % dev.	Exp.	Calc. % dev.	lb./ sq.in.abs.	Sat. gas % dev.	Sat. liq. % dev.	lb./ sq.in.abs.	Sat. gas % dev.	Sat. liq. % dev.	Exp.	Calc. % dev.	Exp.	Calc. % dev.
160	200	0.355	0.045	0.0537	1.3	0.8391	1.0	160.9	−0.6	−16.1	100.3	−0.3	1.2	7.84	−3.6	0.678	1.0
160	300	0.536	0.103	0.0792	0.2	0.8273	0.9	244.5	0.2	−11.3	97.2	0.6	0.6	5.23	−0.2	0.514	−0.7
160	400	0.635	0.162	0.1036	0.2	0.8084	1.1	325.0	0.3	−7.7	94.0	−0.6	0.8	3.92	1.4	0.436	−2.5
160	500	0.694	0.222	0.1274	0.6	0.7814	0.6	399	−0.6	−5.7	90.9	−2.7	2.5	3.12	2.7	0.395	−5.5
160	600	0.732	0.283	0.1484	−0.4	0.7525	0.6	469	−0.5	−1.2	87.6	3.5	−3.7	2.58	5.6	0.375	−6.8
160	700	0.754	0.345	0.1707	0.1	0.7173	0.7	536	0.6	0.5	84.1	1.3	−4.7	2.19	4.3	0.375	−5.9
160	800	0.770	0.409	0.1913	−0.3	0.6799	1.3	601	0.2	2.5	80.5	3.1	−5.5	1.885	5.6	0.387	−7.5
160	900	0.780	0.474	0.2158	0.6	0.6316	0.6	664	0.4	0.9	76.7	1.8	−4.9	1.644	1.5	0.420	−5.4
160	1000	0.784	0.543	0.2388	−0.9	0.5811	1.1	727	0.6	0.7	72.6	0.3	−3.6	1.444	1.0	0.472	−3.0
160	1100	0.778	0.618	0.2909	5.4	0.5099	0.7	779	−1.2	−2.2	68.5	2.1	0.7	1.259	−1.3	0.581	0.3
160	1184 (crit. pt.)	0.713	0.713	0.3678	3.9	0.3678	3.9		−3.0	−3.0	65.0	5.5	5.5	—	—	—	—
Avg. Dev.					1.3		1.1	73.5	0.7	4.7		2.0	3.1		2.7		3.9

TABLE 3. COMPARISON OF EXPERIMENTAL AND CALCULATED K VALUES FOR SEVERAL SYSTEMS

System	Temp. range, °F.	No. of points	Average % deviation in calculated K values Comp. 1	Comp. 2	Data ref.
Carbon dioxide-methane	−100 to 29	78	3.6	4.3	(13)
Carbon dioxide-propane	40 to 160	128	3.3	2.9	(2)
Carbon dioxide-*n*-butane	100 to 220	50	2.8	4.4	(2)
Carbon dioxide-cyclo-hexane	392 to 500	76	3.2	2.8	(14)
Hydrogen sulfide-propane	76 to 201	56	5.9	6.4	(15)
Hydrogen sulfide-*n*-pentane	160 to 340	76	5.7	7.7	(2)
Propane-benzene	160 to 400	64	4.5	6.9	(2)
Methane-nitrogen	−228 to −138	46	5.3	2.7	(16)
Grand total		574	4.3%	4.8%	

Table 2 shows that calculated compressibility factors are generally accurate to about 1% or less except in the critical region where both experimental and computational methods become very sensitive to small errors. The compressibility factors being properties of the mixture as a whole are more accurate than derivative properties such as component fugacities and equilibrium ratios. Deviations for these latter properties, however, do not exceed 8% except for liquid phase fugacities of carbon dioxide at low pressures for which the carbon dioxide concentration is very low. At 200 lb./sq.in.abs. the 16% deviation in the calculated fugacity corresponds to a deviation of the composition of only 0.7 mole % which is about twice the expected experimental error.

Table 3 records average absolute deviations between calculated and experimental equilibrium ratios (y_i/x_i) for eight systems. These binary systems are selected specifically to consist of mixtures of a paraffin hydrocarbon or cyclo-hexane with carbon dioxide, with hydrogen sulfide, with an aromatic (benzene), or with nitrogen. Most methods for predicting equilibrium ratios are known to perform badly with systems of this type which are known to deviate widely from the phase behavior of systems involving only paraffins.

In compiling Table 3 all experimental data appearing in the references cited are used with the following exceptions. The lower reduced temperature limit of the Pitzer tables is 0.8; and whenever the pseudoreduced temperature for the liquid mixture falls below this value, no data are calculated. At the critical point all equilibrium ratios have values of one and are not considered further, but all other data near the critical point are included in the results summarized in Table 3.

These results show for 574 equilibrium ratios an average deviation of 4.55% which compares very favorably with other predictive methods. Overall average deviations for several predictive methods are listed below.

Method	Percent Avg. Dev.
Chao-Seader (3)	7.9
K Chart—A.P.I. (4)	9.0
K Chart—Hadden and Grayson (5)	6.2
K Chart—Cajander et al (6)	5.8
Corr. States—Leland et al. (27, 28, Part I)	10.4
Proposed method	4.6

The deviations reported above are not strictly comparable because different sets of experimental data were used to test the different methods. The first five methods were tested primarily with paraffin mixtures whereas much larger deviations occur for mixtures of the type shown in Table 3. The K chart methods are primarily interpolative techniques. They have been developed from a large body of experimental data, and they become unreliable at temperatures or for components for which experimental data are scarce or nonexistent.

The major advantage of the corresponding states approach is that it requires a minimum of binary data. For the results reported in Table 3 vapor-liquid equilibria data are used only for the purposes of comparing the accuracy of K values except for the carbon dioxide–cyclo-hexane system for which reliable data of other types do not exist. For most of the other systems the k_{ij} values are literature values (1) which have been calculated from saturated liquid density measurements. None of the k_{ij} values used in this work are temperature dependent.

The corresponding states theory developed by Leland et al. (27, 28, Part I) shows an average deviation between calculated and experimental K values of 10.4% based on 140 data points for seven normal paraffins. Average deviations for the equilibrium ratios of individual components vary from 4.3% for *n*-butane to 40.6% for *n*-heptane. The large deviations in the latter case reflect in part at least the difficulty of predicting accurate data at low temperatures for which K values become very small.

The Leland correlation has the advantage of requiring no mixture data. However, it appears that mixture data would be required if compounds such as carbon dioxide, nitrogen, or benzene are present. Apparently no comparisons for systems of this type are available in the literature.

A method recently reported by Lenoir (7) was developed specifically for predicting the phase behavior of carbon dioxide-hydrocarbon mixtures. For this purpose five different charts are used successively to obtain carbon dioxide K values. Several of these charts were prepared from most of the published experimental data for systems of this type.

Table 4 shows a comparison of this method with the corresponding states technique. The deviations for the Lenoir method represent a narrower range of pressures and temperatures than those used in compiling Table 3. Deviations recorded in Table 4 for the corresponding states method cover this same restricted range; and, therefore, these deviations do not coincide with those given in the preceding table. Despite the greater accuracy of the corresponding states method, its major advantage resides in the fact that no experimental vapor-liquid equilibrium data are required. For the three systems compared only mixture second virial coefficients were used to calculate the constant k_{ij}.

COMPARISON OF RESULTS: TERNARY MIXTURES

In both low pressure and high pressure vapor-liquid equilibrium studies accurate sampling and analysis of

Table 4. Comparison of the Accuracy of the *K* Chart Method and the Corresponding States Method for Predicting *K* Values

System	Temp. range, °F.	Carbon dioxide *K* values: No. of points	Carbon dioxide *K* values: % deviation, *K* chart	Carbon dioxide *K* values: % deviation, Corres. states	Hydrocarbon *K* values: No. of points	Hydrocarbon *K* values: % deviation, *K* chart	Hydrocarbon *K* values: % deviation, Corres. states
Carbon dioxide-methane	−65 to 29	17	7.3	1.5	25	3.5	2.0
Carbon dioxide-propane	40 to 160	38	3.9	3.3	30	4.2	1.8
Carbon dioxide-*n*-butane	100 to 220	21	1.6	2.6	10	6.9	3.0

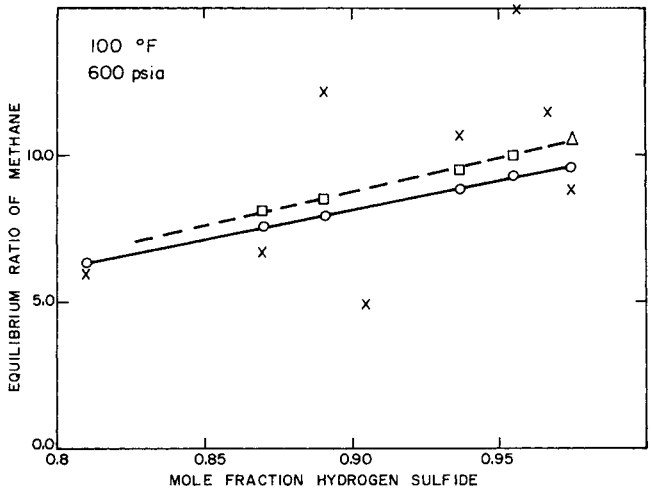

Fig. 1. Comparison of calculated and experimental equilibrium ratios for methane. Methane-carbon dioxide-hydrogen sulfide system at 100°F. and 600 lb./sq.in.abs.

Legend: × Exp. data, (*8*, *9*); △ Exp. data, (*2*); -□---□- Calc. data, Chueh-Prausnitz (*10*); —○—○— Calc. data, this work

phase compositions is a major problem. Comparisons of data for a given binary system studied by more than one investigator usually show compositional differences of at least 1 mole % at the same temperature and pressure. Occasionally deviations of more than 5% are encountered. For this reason much binary experimental data in the literature are questionable in regions of low concentrations for one component.

For ternary mixtures the situation is even more severe because usually at least one of the three components is dilute, that is, below 5 to 10 mole % in at least one phase.

This problem is clearly illustrated by Figures 1 and 2. Figure 1 compares the experimental equilibrium ratios of methane in the methane-carbon dioxide-hydrogen sulfide system (*8*, *9*) at 100°F. and 600 lb./sq.in.abs. with methane *K* values calculated by the corresponding states method and by the method of Chueh-Prausnitz (*10*). Figure 2 is an equivalent comparison at 100°F. and 1200 lb./sq.in.abs. For this system the experimentally determined methane content of the liquid phase is always less than 4 mole % at 100°F. and 600 lb./sq.in.abs. and less than 12 mole % at 1200 lb./sq.in.abs. and the large experimental scatter shown in Figures 1 and 2 corresponds to uncertainties of only ± 0.01 mole fraction methane in the liquid. The large scatter in measured *K* values for methane precludes quantitative assessment of the accuracy of the two predictive techniques. It may only be concluded that both methods, which differ by 7 to 10%, predict equilibrium ratios for methane within the range of experimental error. For the system as a whole, average deviations between experimental *K* values (*8*, *9*) and those calculated by the corresponding states method are 14.8% for methane, 15.8% for carbon dioxide, and 4.3% for hydrogen sulfide. These predictions all fall within the range of experimental error. The good accuracy for the hydrogen sulfide equilibrium ratios reflects the fact that this component existed in fairly large concentrations in both phases under most of the experimental conditions reported.

The following table shows the average deviations between experimental and calculated values for the methane-propane-*n*-pentane system (*11*, *12*).

Pressure range, lb./sq.in.abs.	Temperature range, °F.	No. of points	Average % deviation in equilibrium ratios: Methane	Propane	*n*-Pentane
500-2000	100-220	16	3.4	4.0	11.2

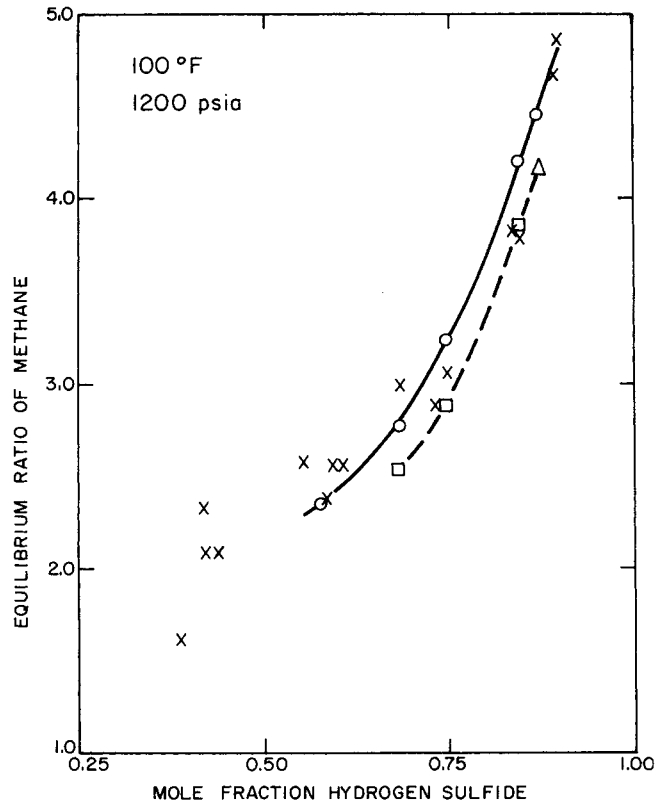

Fig. 2. Comparison of calculated and experimental equilibrium ratios for methane. Methane-carbon dioxide-hydrogen sulfide system at 100°F. and 1200 lb./sq.in.abs.

Legend: × Exp. data, (*8*, *9*); △ Exp. data, (*2*); -□---□- Calc. data, Chueh-Prausnitz (*10*); —○—○— Calc. data, this work

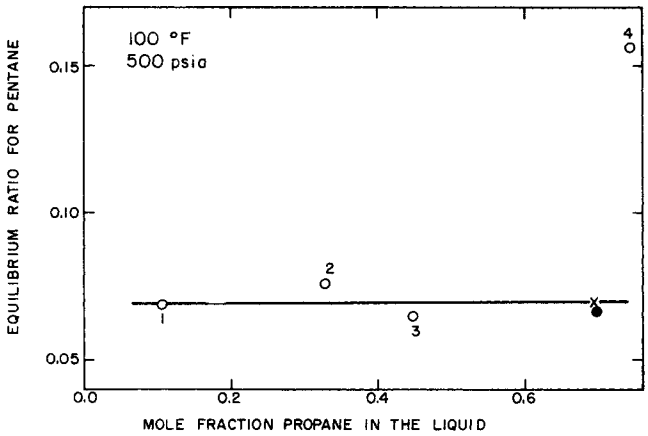

Fig. 3. Equilibrium ratios for *N*-pentane. Methane-propane-*N*-pentane system at 100°F. and 500 lb./sq.in.abs.

Legend: ○ Exp. data, (*11, 12*)
× Calc. data, this work
● Calc. data, *K* Chart (*4*)

The large percentage deviation in pentane K values in the preceding table appears to arise primarily from experimental error. At the conditions reported *n*-pentane is usually rather dilute in the gaseous phase. For this reason, small errors in analyzing for the composition of the gas leads to large errors in the equilibrium ratios. The authors reporting the experimental data also state that it is expected that the behavior of components present in relatively small amounts is not established with sufficient accuracy to be of great engineering utility. (In our opinion these data are, nevertheless, more accurate than corresponding data for the average high pressure ternary vapor-liquid equilibrium study.) Figure 3 illustrates this difficulty. At 100°F. and 500 lb./sq.in.abs. one experimental point deviates drastically from the trend of the remaining data for this system. Two radically different methods for predicting K values, the API K charts (*4*) and the proposed method, both indicate that the trend shown by the solid line is correct. The deviation of about 100% between the experimental datum point no. 4 and the corresponding value indicated by the solid line in Figure 3 arises from a deviation of only 1 mole % in the composition of the gas phase.

CONCLUSIONS AND SUMMARY

The corresponding states method for predicting the thermodynamic properties of fluid mixtures is derived in Part I of this work. In Part II the computational procedure is outlined, and extensive comparisons with experimental data are presented. The proposed theory shows better accuracy than standard K charts and most other methods for predicting phase equilibrium. Current investigations into the density dependence of the scaling parameters and extension of the Pitzer tables to lower reduced temperatures is expected to increase the range of utility and the accuracy of the method still further.

ACKNOWLEDGMENTS

This project has been supported in part by the National Science Foundation through Grant GK-4471. Fujio Kida and Tomoyoshi Yamada have aided with the preparation of the manuscript.

NOTATION

B = second virial coefficient
f = fugacity
g = configuration potential defined by Equations (13), (14), and (15), Part I
H = enthalpy
k_{ij} = binary interaction constant defined by Equation (44)
K = y/x = equilibrium ratio, mole fraction in gas phase/mole fraction in liquid phase
P = pressure
R = universal gas constant
T = temperature
U = internal energy
V = volume
x = mole fraction in liquid phase
y = mole fraction in gas phase
Z = compressibility factor
ω = acentric factor

Subscripts

CM = scaling parameter for mixture
G = gas
L = liquid
i, j, k = components i, j, k respectively
M = mixture
R = reduced property

Superscripts

0 = property for a simple fluid
1 = deviation for an acentric fluid
* = ideal gas property at temperature and pressure of interest

LITERATURE CITED

1. Chueh, P. L., and J. M. Prausnitz, *Ind. Eng. Chem. Fundamentals*, **6**, 492 (1967).
2. Sage, B. H., and W. N. Lacey, "Some Properties of Hydrocarbons," American Petrol. Inst., New York (1955).
3. Chao, K. C., and J. D. Seader, *AIChE J.*, **7**, 598 (1961).
4. "A.P.I. Technical Data Book, Petroleum Refining," American Petrol. Inst., New York (1966).
5. Hadden, S. T., and H. G. Grayson, *Petrol. Refiner (Hydrocarbon Proc.)*, **40(9)**, 207 (1961).
6. Cajander, B. C., H. G. Hipkin, and J. M. Lenoir, *J. Chem. Eng. Data*, **5**, 251 (1960).
7. Lenoir, J. M., *Hydrocarbon Processing*, **46(1)**, 191 (1967).
8. Robinson, D. B., and J. A. Bailey, *Can. J. Chem. Eng.*, **35**, 151 (1957).
9. Robinson, D. B., A. P. Lorenzo, and C. A. Macrygeorgos, *ibid.*, **37**, 212 (1959).
10. Chueh, P. L., and J. M. Prausnitz, "Computer Calculations for High-Pressure Vapor-Liquid Equilibria," Prentice-Hall, Englewood Cliffs, N. J. (1968).
11. Carter, R. T., B. H. Sage, and W. N. Lacey, *Trans. Am. Inst. Min. Met. Engrs.*, **142**, 170 (1941).
12. Dourson, H. R., B. H. Sage, and W. N. Lacey, *Trans. Am. Inst. Min. Met. Engrs.*, **151**, 206 (1943).
13. Donnelly, H. G., and D. L. Katz, *Ind. Eng. Chem.*, **46**, 511 (1954).
14. Krischevsky, I. R., and G. A. Sorina, *Z. Khim. Fiz.*, **34**, 1420 (1960).
15. Kay, W. B., and G. M. Rambosek, *Ind. Eng. Chem.*, **45**, 221 (1953).
16. Brandt, L. W., and L. Stroud, *ibid.*, **50**, 849 (1958).

Manuscript received March 30, 1971; revision received August 11, 1971; paper accepted August 16, 1971.